Generating topological chaos in lid-driven cavity flow

Mark A. Stremler and Jie Chen

Citation: Physics of Fluids (1994-present) **19**, 103602 (2007); doi: 10.1063/1.2772881
View online: http://dx.doi.org/10.1063/1.2772881
View Table of Contents: http://scitation.aip.org/content/aip/journal/pof2/19/10?ver=pdfcov
Published by the AIP Publishing

Generating topological chaos in lid-driven cavity flow

Mark A. Stremler and Jie Chen
Department of Engineering Science and Mechanics, Virginia Polytechnic Institute and State University, Blacksburg, Virginia 24061, USA

(Received 1 May 2007; accepted 18 July 2007; published online 8 October 2007)

Periodic motion of three stirrers in a two-dimensional flow can lead to chaotic transport of the surrounding fluid. For certain stirrer motions, the generation of chaos is guaranteed solely by the topology of that motion and continuity of the fluid. Work in this area has focused largely on using physical rods as stirrers, but the theory also applies when the "stirrers" are passive fluid particles. We demonstrate the occurrence of topological chaos for Stokes flow in a two-dimensional lid-driven cavity without internal rods. This approach to stirring can enhance mixing relative to a "standard" chaos-generating lid-driven cavity flow. © *2007 American Institute of Physics*.
[DOI: 10.1063/1.2772881]

I. INTRODUCTION

It has been shown that one can establish a quantitative lower bound on the complexity of a two-dimensional stirred flow simply by examining the motion of the boundaries.[1] If the fluid domain contains a sufficient number of stirring rods[2] that are moved about appropriately, the topology of the time-dependent rod motions guarantees that at least some of the fluid is subjected to exponential stretching and folding. The prediction and analysis of this "topological chaos" is based on the Thurston-Nielsen (TN) theory,[3,4] a powerful collection of mathematical tools for analyzing two-dimensional dynamical systems.

Much of the existing work that uses this topological approach to fluid mixing has focused on systems in which the stirring is produced by three solid rods inserted in the flow. Consider, for example, viscous flow in a circular domain that is driven by the motion of three cylindrical rods intersecting the domain. In this example the stirrer motions take place in two steps. First, the right rod and the center rod interchange position by simultaneously moving clockwise along a circular path, as shown in Fig. 1(a). During this motion, the left rod remains stationary. We will refer to this stirrer motion as R_+. Next, the left and center rods interchange position by moving along a circular path either clockwise, as shown in Fig. 1(b), or counterclockwise, as shown in Fig. 1(c), while the right rod remains stationary. We will refer to these stirrer motions as L_+ and L_-, respectively. These two steps then repeat, and after six steps the rods return to their original positions, giving one full period of the stirrer motions. These stirring protocols have been examined experimentally in viscous flow[1] and numerically in both potential flow[5] and Stokes flow.[5,6] Similar stirring protocols can be achieved by holding two of the rods fixed and moving the third rod about these two in a figure-eight or epicyclic pattern.[5,7] A recent variation on this system combines figure-eight motion of one rod with rotation of two "baffle" rods.[8]

Topological chaos refers to complexity in the flow that cannot be removed by continuous perturbation of the fluid while holding the boundaries (i.e., the rods) fixed. For the example in Fig. 1, the occurrence of topological chaos depends on whether the second rod interchange is done in the clockwise or counterclockwise direction. It is the direction of interchange that is important, not the specific shape of the path. If this interchange is counterclockwise, so that the stirrer motion consists of R_+ followed by L_-, then chaos is "built in" the system in a way that does not depend on the detailed dynamics of the rods or the fluid. That is, in this case the stirred flow is topologically equivalent (i.e., isotopic) to a chaotic *pseudo-Anosov* (pA) map that has a dense collection of periodic orbits and a Markov partition with irreducible transition matrix A. Except for a finite number of singularities, this pA map stretches everywhere in the unstable direction(s) by a factor $\lambda > 1$, the dominant eigenvalue of A, and contracts everywhere in the stable direction(s) by a factor $1/\lambda$. This complicated behavior is preserved under isotopy,[9] i.e., under any continuous deformation in which the stirrers remain fixed, so that in a subdomain of the real fluid this stirring motion produces exponential stretching at a rate that is at least λ. (See, e.g., Refs. 1 and 10 for a more complete discussion of isotopy in a fluid mechanics context.) The size of the subdomain is not predicted by the TN theory, but the experimental results reproduced in Fig. 1(f) indicate that this region is on the scale of the stirrer motions. Thus, if a stirrer motion is of pA type, a small amount of rough topological data enables prediction of a quantitative lower bound on complexity in the dynamics of the flow. The existing work demonstrates that this prediction is of practical importance in almost all cases considered thus far, the one exception being steady, three-dimensional flow in a duct with a "stirring rod" insert.[11]

If the second interchange in the above example is instead clockwise, so that the stirrer motion consists of R_+ followed by L_+, then the net effect of this motion is simply to twist the fluid around the rods. *Finite order* motions such as this are topologically trivial, and the TN theory gives no lower bound on complexity in the resulting flow. Figure 1(e) shows that the corresponding fluid motion can be nontrivial, and even chaotic, but this complexity is due to the dynamics of the flow, not the topology of the boundary motions, and can thus be removed by varying parameters such as the shape of the

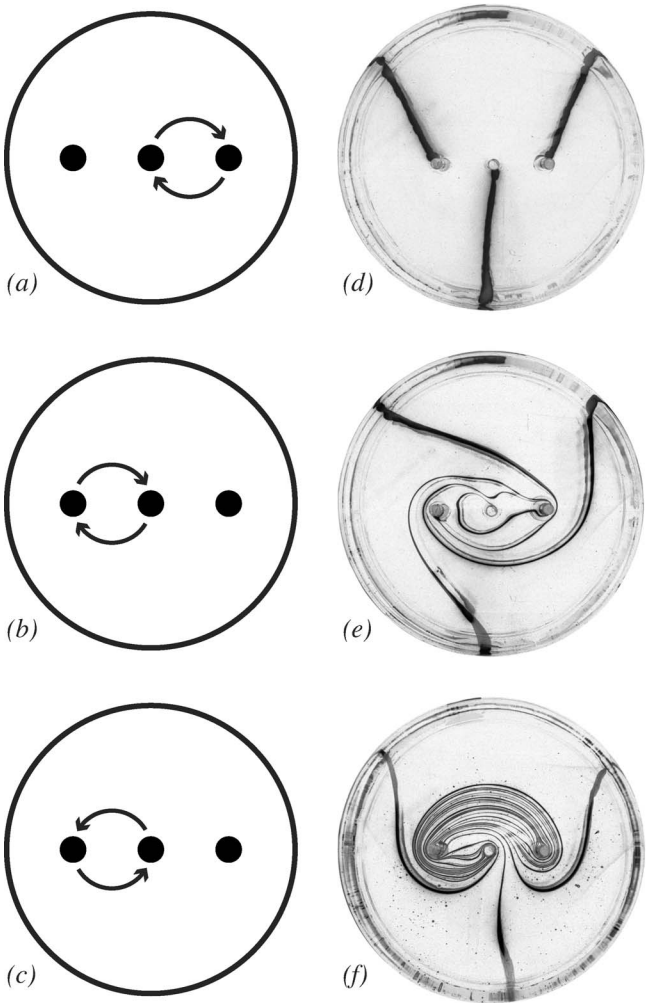

FIG. 1. Stirring a viscous fluid with three rods, from Ref. 1. The rods are orthogonal to the image plane. Panels (a)–(c) show the rod interchanges, or stirrer motions, (a) R_+, (b) L_+, and (c) L_-. Panels (d)–(f) show experimental dye visualization images for (d) the initial dye configuration, (e) a finite order motion after three periods of the flow, and (f) a pseudo-Anosov motion after three periods of the flow.

domain or the speed of the boundaries. Furthermore, qualitative comparison of the experimental results in Fig. 1 shows the advantage of using a pA motion to stir the fluid. These two stirring protocols are energetically equivalent, but the stirring produced with the pA motion is significantly more efficient than that with the finite order motion.

The TN theory does not require that the stirrers producing topological chaos be solid rods. For example, when three point vortices are allowed to interact dynamically in a singly-periodic domain, some of the resulting vortex motions are of pA type.[12] In fact, the stirrers examined with the TN theory need not be driving the flow at all, but merely be passive particles (or groups of particles) that happen to experience the appropriate trajectories. These passive periodic structures have been termed *ghost rods*.[13]

Existing analyses of topological chaos in a fluid with ghost rods consider two cases. In one case, a single rod in a circular domain is moved along either a figure-eight or epicyclic trajectory. The stirrer motions generated by this single rod are topologically trivial. However, each of these trajectories produce multiple elliptic islands that act as ghost rods in the flow. The stirring motions generated by the combination of the solid rod and at least two ghost rods can be of pA type, and the results are similar to those in which a single rod moves about two fixed solid rods.[5,7] The other case considers sine flow on a torus, in which the periodic points alone generate a stirring motion of pA type.[14] This sine flow is quite useful for analysis, but has no clear physical analog.

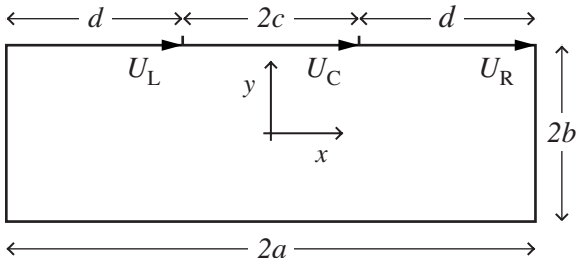

FIG. 2. Geometry of a lid-driven cavity with the top boundary split into three segments. The tangential velocities of the left, center, and right segments are given by U_L, U_C, and U_R, respectively. The geometry shown here has an aspect ratio $\alpha=a/b=3$ and a boundary length ratio $\beta=2c/d=1$.

In this paper, we use a model of Stokes flow in a two-dimensional lid-driven cavity to demonstrate that passively advected periodic points can be made to follow trajectories that guarantee the presence of topological chaos in a practical flow without any internal rods. In Sec. II we discuss the details of the lid-driven cavity flow being considered, and in Sec. III we examine the role of topological chaos in this flow. We conclude in Sec. IV. Preliminary results of this work were presented at the 59th Annual Meeting of the American Physical Society Division of Fluid Dynamics.[15]

II. THE LID-DRIVEN CAVITY FLOW

The two-dimensional lid-driven cavity system has been used numerous times to generate chaotic motion in a viscous fluid (see, e.g., Refs. 16–18). Flow inside the cavity is driven by time-dependent tangential motion of the boundaries. In the standard lid-driven cavity, these tangential velocities are taken to be uniform along the entire length of each boundary. In our system we drive only the top boundary, which we split into three segments as shown in Fig. 2, with the tangential velocity of each boundary segment assigned independently. Not only does this system provide a basis for examining topological chaos with ghost rods, but it has also been used recently to model secondary flow in microchannels with surface patterns[19] and electro-osmotic flow in microchannels with varying surface charge.[20]

For Stokes flow in the two-dimensional rectangular domain shown in Fig. 2 with $|x|\leqslant a$ and $|y|\leqslant b$, the stream function $\psi(x,y)$ satisfies the two-dimensional biharmonic equation

$$\nabla^2\nabla^2\psi(x,y)=0 \tag{1a}$$

with the boundary conditions

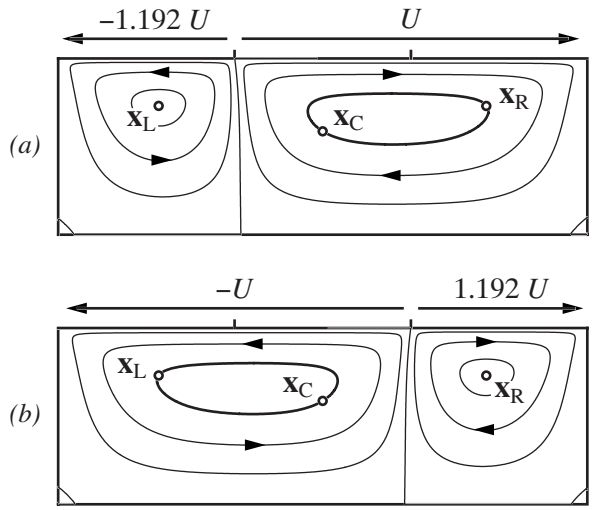

FIG. 3. Representative streamlines in the steady flow generated by the boundary velocity distributions (a) $U_C=U_R=U>0$ and $U_L\approx-1.192U$, which produces motion analogous to R_+ in Fig. 1(a), and (b) $U_L=U_C=-U<0$ and $U_R\approx1.192U$, which produces motion analogous to L_- in Fig. 1(c). The periodic points used to determine the velocity ratio are labeled $\mathbf{x}_L,\mathbf{x}_C,\mathbf{x}_R$.

$$x=\pm a:\quad \psi=0,\quad \partial\psi/\partial x=0,$$

$$y=b:\quad \psi=0,\quad \partial\psi/\partial y=V(x), \tag{1b}$$

$$y=-b:\quad \psi=0,\quad \partial\psi/\partial y=0,$$

where the top boundary velocity is given by the piecewise constant distribution

$$V(x)=\begin{cases} U_L & \text{for } -(c+d)\leqslant x<-c,\\ U_C & \text{for } -c\leqslant x\leqslant c,\\ U_R & \text{for } c<x\leqslant c+d. \end{cases} \tag{1c}$$

We solve for $\psi(x,y)$ using a method discussed by Meleshko[21,22] that has its origins in the work of Lamé. This approach is similar to obtaining a Fourier series representation, but instead of assuming all higher-order terms are zero the asymptotic behavior of these terms is approximated. Use of this method makes it possible to accurately represent the discontinuities in the boundary velocity. Our objective here is to demonstrate that one can generate topological chaos in a lid-driven cavity by establishing a flow similar to that shown in Fig. 1(f). For the sake of this discussion we will focus on the particular cavity geometry in Fig. 2 with aspect ratio $\alpha=a/b=3$ and boundary length ratio $\beta=2c/d=1$, for which $b=c$.

Choosing $U_C=U_R=U>0$ and $U_L<0$ gives a flow such as that illustrated in Fig. 3(a). In order to produce a "rod interchange" similar to the stirrer motion R_+ in Fig. 1(a), we look for a velocity ratio U_L/U that satisfies the following two conditions: (i) three points exist in the flow at the positions $\mathbf{x}_L=(-x_1,y_1)$, $\mathbf{x}_C=(0,y_0)$, $\mathbf{x}_R=(x_1,y_1)$, such that $\mathbf{x}_L$ is a stagnation point in the flow, and $\mathbf{x}_C$ and $\mathbf{x}_R$ lie on the same streamline; and (ii) the points $\mathbf{x}_C$ and $\mathbf{x}_R$ exactly change positions after time T. We will work in terms of a dimensionless "pulse time" $\tau=|U|T/(2b)$. For the chosen geometry,

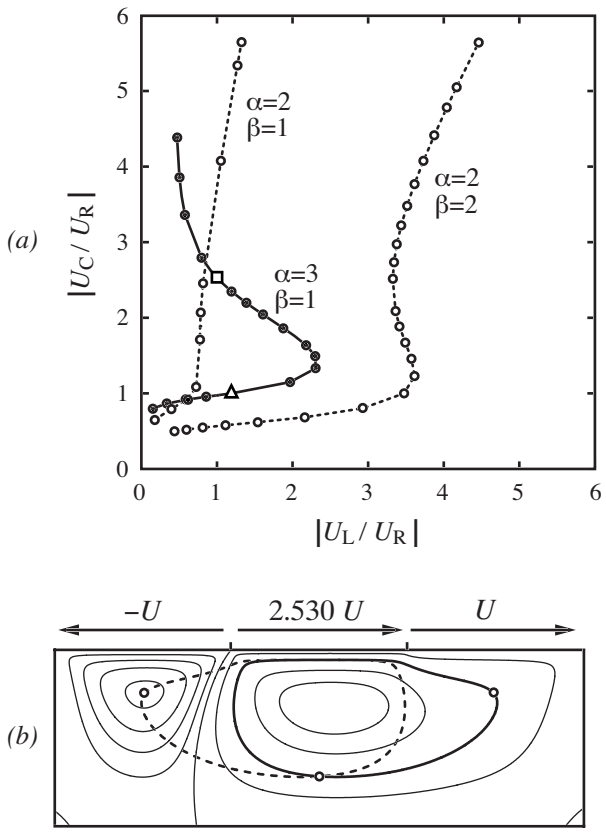

FIG. 4. (a) Velocity ratios that satisfy conditions (i) and (ii) in Sec. II for various choices of aspect ratio α and boundary length ratio β. The triangle △ marks the case shown in Fig. 3. (b) Sample streamlines (solid lines) and the periodic points $\mathbf{x}_L,\mathbf{x}_C,\mathbf{x}_R$ for the case $\alpha=3$, $\beta=1$, $-U_L=U_R=U$, $U_C\approx2.530U$. This case is marked by the square □ in (a). The dashed line is the streamline passing through $\mathbf{x}_L$ and $\mathbf{x}_C$ for $U_C\approx-2.530U$, with all other parameters the same.

these two conditions are satisfied by taking $U_L/U\approx-1.192$ and $\tau\approx5.379$. We will refer to this pulse of the flow, shown in Fig. 3(a), as the *lid-driven motion* R_+.

Producing the analog of a left "rod interchange" is accomplished by taking $U_L=U_C=-U$ with $U_R/U\approx1.192$. The point $\mathbf{x}_R$ is now a stagnation point, and the points $\mathbf{x}_L$ and $\mathbf{x}_C$ exchange positions after time $\tau\approx5.379$. If $U>0$, $\mathbf{x}_L$ and $\mathbf{x}_C$ orbit in a counterclockwise direction, as shown in Fig. 3(b); we refer to one pulse of this flow as the *lid-driven motion* L_-. If instead $U<0$, we generate the lid-driven motion L_+.

Our lid-driven pA flow thus consists of periodically and instantaneously switching between the steady lid-driven motion R_+ and the steady lid-driven motion L_-. Each of these individual motions persists for time τ, so the flow is time periodic with a period $\tau_f=2\tau$. The reader can easily verify that the points starting at $\mathbf{x}_L,\mathbf{x}_C,\mathbf{x}_R$ return back to their initial positions after three periods of the flow, so that these "ghost rods" have a period $\tau_r=6\tau$. This flow is obviously a very specific case; it appears that once the geometry (i.e., the aspect ratio α and boundary length ratio β) is given, conditions (i) and (ii) above are satisfied for only one value of U_L/U when we require $U_C=U_R=U$. Other cases can be found if we allow each boundary velocity to be assigned independently or if we change the geometry. Figure 4 documents several parameter values for which the three desired periodic points

exist. For example, if we again take $\alpha=3$ and $\beta=1$ but now specify that $-U_L=U_R=U\neq|U_C|$, the conditions are met when $|U_C|/U\approx 2.530$ and $\tau\approx 2.921$; streamlines for this case are shown in Fig. 4(b). In general, the existence and topology (but not necessarily the symmetry) of these periodic orbits will persist under slight parametric perturbation. A more in-depth investigation into the effect of perturbation on the existence of "ghost rods" in a lid-driven cavity flow requires careful consideration of the structure of such a rod. We will pursue this line of research in a subsequent manuscript.

III. TOPOLOGICAL CHAOS IN THE LID-DRIVEN CAVITY

We focus our attention on the case illustrated in Fig. 3 with one period of the flow consisting of the lid-driven motion R_+ followed by the lid-driven motion L_-. In this case there exist three periodic points in the flow (viz. $\mathbf{x}_L$, $\mathbf{x}_C$, and $\mathbf{x}_R$) that travel in a pA motion analogous to that of the physical rods used in Ref. 1.

The Thurston-Nielsen theory gives a quantitative lower bound on the topological entropy of a flow; we will refer to this lower bound as h_{TN}. When the flow is of pA type, the theory guarantees that $h_{\mathrm{TN}}>0$. Topological entropy is the logarithm of the maximum stretching rate in the flow. Thus, when the flow is of pA type, at least a portion of the fluid is stretched exponentially in time, so that the flow contains chaos due to the topology of the boundary motions.

Since the foundation for this analysis is the motion of boundaries, the appropriate view of our cavity flow is the following: If R is the domain contained within the rectangular cavity boundary, define $R^0=R-\{\mathbf{x}_L,\mathbf{x}_C,\mathbf{x}_R\}$. The pA flow that consists of periodically switching between the lid-driven motions R_+ and L_- generates a mapping $f:R^0\rightarrow R^0$, and f is isotopic to the mapping for the flow shown in Fig. 1. That is, these two flows are topologically equivalent because the motions of the "stirring rods" are topologically equivalent. The predicted lower bound on topological entropy is the same for all flows that are isotopic to one another. Thus, as shown in Ref. 1, $h_{\mathrm{TN}}=\ln\left[\frac{1}{2}(3+\sqrt{5})\right]\approx 0.96$, so that the number of periodic points of f and the length of nontrivial material lines in R^0 both grow at least as fast as $\exp(nh_{\mathrm{TN}})$ under iteration, where n enumerates the period of the flow.

This prediction of exponential stretching applies to topologically nontrivial material lines in the flow, such as loops that encircle exactly two of the stirring rods or lines that join a stirring rod with the outer boundary. The actual topological entropy of the flow, h_f, can be determined by computing the rate at which these nontrivial lines are stretched.[23] We estimate that $h_f\approx 1.92$ for this lid-driven cavity flow by computing the stretching rate for the two material lines shown in Fig. 5(a). The evolution of these lines is shown in Fig. 5 for three periods of the flow; the estimate of h_f converges after roughly 3–4 periods of the flow.

Physically, one can think of the TN theory as giving the stretching rate for a taut elastic cord that joins two of the stirring rods. For a pA motion the cord will be tangled around the three rods in a way that stretches it exponentially in time. A material line will experience this stretching *plus* that generated by the additional complexities of the flow between the rods, causing the entropy of the flow to be greater than (or possibly equal to) the lower bound predicted by the TN theory. The more the flow is dominated by the motion of the rods, the better the prediction of the lower bound. In this lid-driven cavity flow, $h_f\approx 2h_{\mathrm{TN}}$, a substantial increase in entropy over the theoretical lower bound. This large value of the entropy suggests that there is at least one other unidentified periodic orbit, or ghost rod, in the flow that is producing nontrivial stirring in addition to that of our three "intentional" rods. In principle, there exist orbits in the flow that make the predicted value for h_{TN} arbitrarily close to h_f, although these orbits may be quite long and complicated.[13,24]

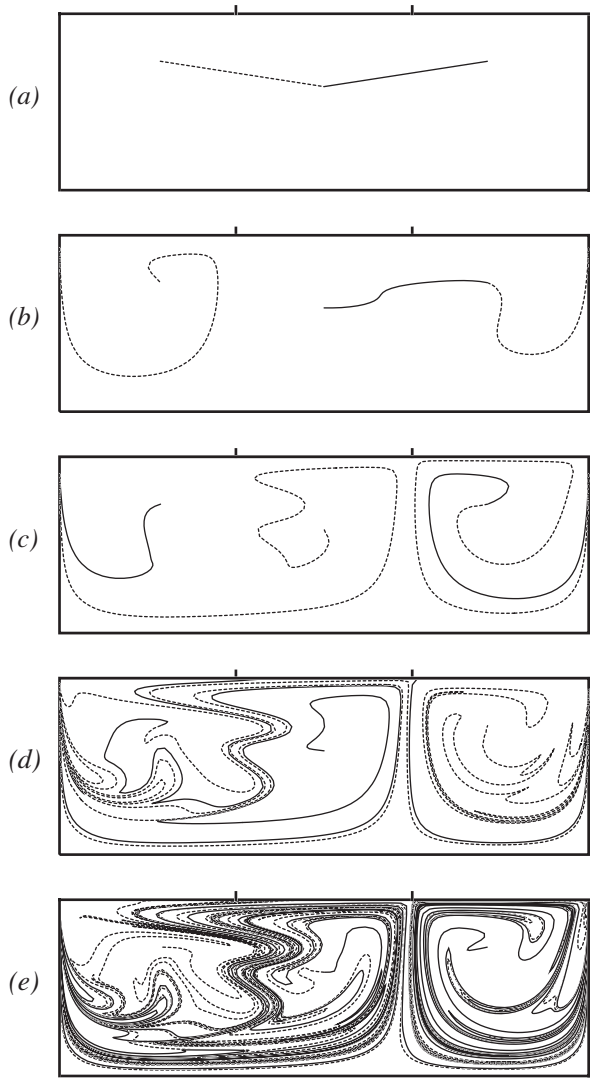

FIG. 5. Stretching of material lines joining points $\mathbf{x}_L$ and $\mathbf{x}_C$ (dashed line) and points $\mathbf{x}_C$ and $\mathbf{x}_R$ (solid line). (a) Initial line positions at time $t=0$. [(b)–(e)] Deformation of the lines by the pA lid-driven cavity flow at times (b) τ, (c) $2\tau=\tau_f$, (d) $2\tau_f$, and (e) $3\tau_f$.

As material lines are stretched by a pA motion, they converge to the unstable foliations in the flow. Since both Fig. 1(f) and Fig. 5(e) have the same underlying pA motion, one expects the patterns of the stretched material lines to be similar, even though the initial lines are different. There are indeed similarities, particularly at the cusp where fluid is

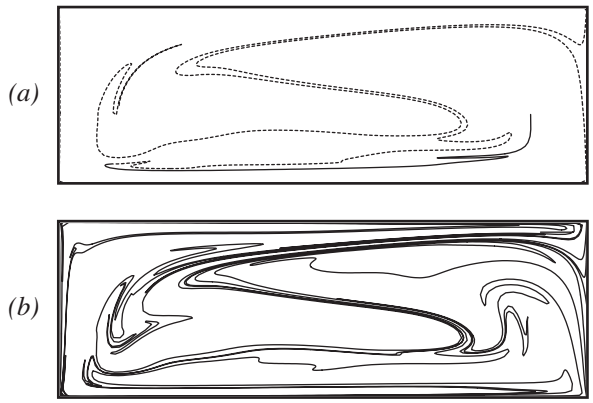

FIG. 6. Stretching of the material lines (a) shown in Fig. 5(a) and (b) along $y=0$ using the standard lid-driven motion described in the text for time $t=3\tau_f$. This motion requires the same input power as that in Fig. 5(e).

drawn between the center and right rods. However, there are also several apparent differences. In Fig. 5 it appears that segments of material line terminate at each of the top corners. The structure of this flow continually drives material lines to the top boundary at the separating streamline (see Fig. 3) and then along that boundary to the top corners. This motion causes a very dense packing of material lines along the top boundary that we do not resolve in Fig. 5. Thus, the striations that are layered above all three rods in Fig. 1(f) are not clear in Fig. 5(e). Perhaps more importantly, in this lid-driven cavity flow material lines are stretched vertically between the left and center rods, which does not happen in the case with physical rods. In the lid-driven cavity, the fluid around the stationary "ghost rod" experiences significant rotation, which adds to the complexity of the underlying structure.

Finally, for comparison we consider mixing in a "standard" lid-driven cavity flow.[16–18] In the first half of this motion, we drive the entire top boundary of the cavity to the right with a (constant) speed V. In order to generate a motion that is energetically equivalent to the case with split boundaries, we operate for the same time $\tau \approx 5.379$ with a boundary velocity $V=1.305U$ chosen such that the input power is the same in both cases; that is,[25]

$$P/\mu = \left[-1.192U \int_{-a}^{-c} \left. \frac{\partial u}{\partial y} \right|_{y=b} \mathrm{d}x + U \int_{-c}^{a} \left. \frac{\partial u}{\partial y} \right|_{y=b} \mathrm{d}x \right]_{\text{split}} \tag{2a}$$

$$= \left[V \int_{-a}^{a} \left. \frac{\partial u}{\partial y} \right|_{y=b} \mathrm{d}x \right]_{\text{full}} . \tag{2b}$$

In the second half of this motion, the entire bottom boundary is driven to the right with the same speed V for the same time τ.

After three periods of this flow, the lines in Fig. 5(a) are deformed as shown in Fig. 6. Obviously, much less stretching has taken place here than in Fig. 5(e). In Fig. 6(a), a large portion of the solid line lies within an elliptic island, so we have also included the stretching of a horizontal line to give a more complete picture of the stirring achieved by this case. We have estimated the topological entropy for this flow to be $h_g \approx 0.92$. Since $h_g > 0$, there must exist a set of ghost rods in this flow that generate a pA motion.[13,24] However, since $h_g < h_{\text{TN}}$, this motion is less efficient at stirring the fluid than the above split-boundary motion. In fact, any split-boundary cavity flow with periodic points exhibiting the necessary R_+, L_- motions is *guaranteed* to produce a greater stretching rate than any standard cavity flow with $h_g < h_{\text{TN}}$.

IV. CONCLUSIONS

A lid-driven cavity with split boundaries can generate "ghost rods" within the cavity that "stir" the fluid in a pseudo-Anosov motion. For the case we have examined, the trajectories of these ghost rods are analogous to those of the physical stirring rods shown in Fig. 1. The existence of this pseudo-Anosov motion guarantees the presence of chaotic transport in the flow and, through the Thurston-Nielsen theory, a quantitative lower bound on the stretching rate for topologically nontrivial material lines. Thus, important information regarding stirring efficiency (and hence mixing) in this flow can be determined *a priori* by merely finding the appropriate periodic points.

The results presented here are valid for Stokes flow in a two-dimensional lid-driven cavity with particular choices for the boundary velocities. The predictions of the Thurston-Nielsen theory for this system are based on the existence of the ghost rods, which depends on the details of the fluid dynamics. This influence of the dynamics on analysis of the topological kinematics is in contrast to systems with physical rods such as considered in Ref. 1 and shown in Fig. 1. For those systems in which physical rods perform the stirring, the topology of the imposed rod motion guarantees the presence of chaotic transport in the surrounding fluid. This prediction is not subject to changes in the rod velocities or the fluid rheology, for example, although the details of the mixing will depend on these parameters. For systems in which ghost rods perform the stirring, consideration must be given to the effect of perturbation on the rods. We have shown that the requisite ghost rods exist in our lid-driven cavity flow for various choices of cavity geometry. It is also expected that these periodic orbits will persist under small perturbations in boundary velocity ratios and pulse time; we have confirmed this expectation for some test cases.

The success of this approach to stirring enhancement in a lid-driven cavity flow suggests that topological chaos and the Thurston-Nielsen theory be considered in the analysis of other fluid mixing systems without physical stirring rods.

ACKNOWLEDGMENTS

This manuscript was being edited in Norris Hall when the shooting began there on the morning of April 16, 2007 and is dedicated to the memory of Kevin P. Granata and Liviu Librescu, colleagues who lost their lives in that tragedy.

The authors thank P. L. Boyland and J.-L. Thiffeault for numerous insightful discussions. This material is based upon work supported by the National Science Foundation under Grant Nos. DMS-0701126 and CBET-0507903.

[1]P. L. Boyland, H. Aref, and M. A. Stremler, "Topological fluid mechanics of stirring," J. Fluid Mech. **403**, 277 (2000).
[2]Three rods are required for bounded or unbounded two-dimensional flow in the plane. As discussed in Ref. 14, if the flow is on a cylinder (i.e., is a singly-periodic, two-dimensional flow) or is on a torus (i.e., is a doubly-periodic, two-dimensional flow), then only two stirring rods are required.
[3]W. Thurston, "On the geometry and dynamics of diffeomorphisms of surfaces," Bull., New Ser., Am. Math. Soc. **19**, 417 (1988).
[4]A. Casson and S. Bleiler, *Automorphisms of Surfaces after Nielsen and Thurston* (Cambridge University Press, New York, 1988).
[5]M. D. Finn, S. M. Cox, and H. M. Byrne, "Topological chaos in inviscid and viscous mixers," J. Fluid Mech. **493**, 345 (2003).
[6]A. Vikhansky, "Simulation of topological chaos in laminar flows," Chaos **14**, 14 (2004).
[7]M. J. Clifford and S. M. Cox, "Smart baffle placement for chaotic mixing," Nonlinear Dyn. **43**, 117 (2006).
[8]B. J. Binder and S. M. Cox, "A mixer design for the pigtail braid," Fluid Dyn. Res. (in press).
[9]M. Handel, "Global shadowing of pseudo-Anosov homeomorphisms," Ergod. Theory Dyn. Syst. **5**, 373 (1985).
[10]J.-L. Thiffeault and M. D. Finn, "Topology, braids and mixing in fluids," Philos. Trans. R. Soc. London, Ser. A **364**, 3251 (2006).
[11]M. D. Finn, S. M. Cox, and H. M. Byrne, "Chaotic advection in a braided pipe mixer," Phys. Fluids **15**, L77 (2003).
[12]P. Boyland, M. Stremler, and H. Aref, "Topological fluid mechanics of point vortex motions," Physica D **175**, 69 (2003).
[13]E. Gouillart, J.-L. Thiffeault, and M. D. Finn, "Topological mixing with ghost rods," Phys. Rev. E **73**, 036311 (2006).
[14]M. D. Finn, J.-L. Thiffeault, and E. Gouillart, "Topological chaos in spatially periodic mixers," Physica D **221**, 92 (2006).
[15]J. Chen and M. A. Stremler, "Topological chaos in cavities and channels," Bull. Am. Phys. Soc. **51**, 152 (2006).
[16]W. Chien, H. Rising, and J. M. Ottino, "Laminar mixing and chaotic mixing in several cavity flows," J. Fluid Mech. **170**, 355 (1986).
[17]C.-W. Leong and J. M. Ottino, "Experiments on mixing due to chaotic advection in a cavity," J. Fluid Mech. **209**, 463 (1989).
[18]P. G. M. Kruijt, O. S. Galaktionov, P. D. Anderson, G. W. M. Peters, and H. E. H. Meijer, "Analyzing mixing in periodic flows by distribution matrices: mapping method," AIChE J. **47**, 1005 (2001).
[19]A. D. Stroock and G. J. McGraw, "Investigation of the staggered herringbone mixer with a simple analytical model," Philos. Trans. R. Soc. London, Ser. A **362**, 971 (2004).
[20]S. Qian and H. H. Bau, "Theoretical investigation of electro-osmotic flows and chaotic stirring in rectangular cavities," Appl. Math. Model. **29**, 726 (2005).
[21]V. V. Meleshko and A. M. Gomilko, "Infinite systems for a biharmonic problem in a rectangle," Proc. R. Soc. London, Ser. A **453**, 2139 (1997).
[22]V. V. Meleshko and A. M. Gomilko, "Infinite systems for a biharmonic problem in a rectangle, further discussion," Proc. R. Soc. London, Ser. A **460**, 807 (2004).
[23]S. Newhouse and T. Pignataro, "On the estimation of topological entropy," J. Stat. Phys. **72**, 1331 (1993).
[24]P. L. Boyland, "Topological methods in surface dynamics," Topol. Appl. **58**, 223 (1994).
[25]Note that the velocity gradients in Eq. (2) become infinite at discontinuities in the boundary velocity. Thus these integrals exclude an ϵ-neighborhood around the points $x=\pm a, \pm c$, and the value of V is determined by considering the limit $\epsilon \to 0$.